Pilot-scale investigation of flowrate and temperature influence on the performance of hollow fiber forward osmosis membrane in osmotic concentration process

Rem Jalab [a], Abdelrahman M. Awad [a], Mustafa S. Nasser [a,*], Joel Minier-Matar [b], Samer Adham [b]

[a] *Gas Processing Centre, College of Engineering, Qatar University, Doha, Qatar*
[b] *ConocoPhillips Global Water Sustainability Centre, Qatar Science & Technology Park, Doha, Qatar*

A B S T R A C T

Forward osmosis (FO) relying on the osmotic pressure difference across semi-permeable membrane draws permeate by the effect of saline draw solution (DS) turning diluted and leaving the feed solution (FS) concentrated. However, the energy intensive step of DS recovery makes FO a challenging process. The energy benefit of FO emerges when recovery step is obviated and FO is applied as an osmotic concentration (OC) process. OC implementations for volume reduction are still at bench-scale and the investigation at larger scale is among the breakthroughs. In this paper, the performance of hollow fiber (HF) membrane in pilot-scale OC process for reducing volume of feed was investigated. The impact of operating conditions such as flowrates and temperature was evaluated. FS and DS flowrates of 1.35 and 0.35 L.min⁻¹ respectively are optimum conditions with 75% feed recovery and 1.90 LMH water flux. Reverse solute flux increased at higher flowrates. Results indicated the role of high DS flowrate and temperature in improving the performance. DS flowrate of 0.35 L.min⁻¹ at constant FS flow of 1.10 L.min⁻¹ and 27 °C was most suitable for achieving 84.5% feed recovery and 1.82 LMH water flux. Above all, the long-term performance of OC pilot-plant was demonstrated through 48 h of continuous operation where stable flux trend at an average water flux of 1.66 LMH was successfully achieved. Lastly, the permeability coefficients of HF membrane were enhanced at higher temperature.

1. Introduction

Osmotic concentration (OC) is an application of the low-energy membrane-based technology named forward osmosis (FO). Basically, FO is featured by the exploitation of natural osmosis phenomenon for the water transport across a semi-permeable membrane [1–3]. Through the membrane barrier, the fresh water (permeate) is transferred from low osmotic pressure feed solution (FS) to high osmotic pressure solution with high solute concentration known as draw solution (DS) [4]. It has been claimed that FO process, relying on natural osmosis, consumes less energy when compared with pressure driven processes such as reverse osmosis (RO) for certain application where DS recovery is obviated. As more water permeates through the membrane, DS salinity decreases and net driving force reduces demanding the recovery of DS. Therefore, FO is described by being two steps process including the membrane separation followed by DS re-concentration step as shown in Fig. 1. The DS recovery is commonly achieved through reverse osmosis

(RO), nanofiltration (NF) [5] or thermal separation processes [6]. While the separation stage requires small energy amount, the DS recovery is a high-energy step making FO a challenging process [7]. Nevertheless, FO can beat the pressure-driven processes in terms of costs when FO implementation is prioritized to applications where DS regeneration is not compulsory [2,8].

In the OC process, the volume of feed water is reduced while the DS is diluted, as fresh water permeates from the feed stream to the DS stream. Therefore, DS recovery step can be eliminated for the OC applications when recovering water product is not a concern and the aim is having the concentrated feed at reduced volume. FO operating as OC process is best suited for volume reduction of wastewater stream from oil and gas wells' drilling activities [9,10]. OC process was demonstrated at bench-scale in two research projects for the volume reduction of O&G wastewater [11,12]. The investigation of Hickenbottom et al. [11] for OC at bench- scale level demonstrated an 80% volume reduction of drilling mud and fracturing wastewater. In another bench-scale study,

Minier-Matar et al. [12,13] demonstrated the successful implementation of OC process for 50% volume reduction of produced and process water effluent. In spite of the promising outcomes, OC for the purpose of wastewater volume reduction has not been investigated at larger scale.

The high solute rejection [14], low fouling propensity [15] and low energy consumption are all key attributes of FO technology as compared to pressure driven process (RO). However, FO process is still facing some critical operational problems in the areas of concentration polarization inside and around the membrane, reverse solute flux and membrane fouling [7]. In fact, concentration polarization incidence is related to the difference in concentration between FS and DS across the membrane. FO-based processes experience both external and internal concentration polarization (ECP, ICP) existing in porous support layer and surface of membrane's active layer respectively [16]. Concentration polarization crucially reduces the osmotic pressure gradient across the membrane's active layer and then decreases the water flux (volume of permeated water over the membrane area per specific time). Furthermore, the flux decline is due to the reverse solute flux (RSF) which is the diffusion of salts from DS side through the membrane to FS side [14]. Consequently, these challenges might be the reasons for the rarely conducted large-scale testing of the technology under conditions representative to the real-life applications [4].

Despite the growth of interest in FO research in the past 10 years, there exists only few pilot and demonstration-scale installations with ten identifiable commercial membranes suppliers shown in Table 1 [17]. Other studies were reported using RO membranes or bespoke hand-cast FO membrane modules [18,19]. Commonly, the FO membranes manufacturing materials are either the cellulose triacetate (CTA) or the polyamide and polyelectrolyte based thin film composite (TFC) [20,21]. The diverse types of FO membranes in the market comprise the flat sheet (FSh), plate and frame (PF), spiral wound (SWo) and hollow fiber (HF) configurations [22–25]. The flat sheet and spiral wound FO membranes manufactured by Fluid Technology Solutions (USA) are featured with the high fouling and abrasion resistance rendering them ideal for the treatment of complex streams such as landfill leachate, specifically the spiral wound membranes manufactured under the industrial standards are capable of treating all contamination levels in any wastewater streams [22]. Porifera declared that its manufactured plate and frame modules are modules operating in co-current and counter current modes and of high water flux, efficiency reaching 95% and low head loss [25]. Whereas, the HF made membranes produced by Toyobo, Aquaporin and Aromatec are described by the high packing density of the fibers stacked in a pressure vessel, the increased water permeability and ions rejection [26]. Besides, the HF module configuration alleviates the internal concentration polarization (ICP) problems from the eliminated porous support layer [27].

Table 1
Some of existing FO membranes suppliers.

FO Membrane Suppliers		Origin	FO Membrane Configuration
	Aquaporin	Denmark	Flat sheet & hollow fiber
	Porifera	USA	Flat sheet & plate and frame
	Trevi Systems	USA	Proprietary membrane
	Toyobo	Japan	Hollow fiber
	Fluid Technology Solutions (FTS) (previously named HTI)	USA	Flat sheet & spiral wound
	Berghof Membrane technology	Germany	Tubular configuration membranes
	Sterlitech	USA	Flat sheet
	Koch Membrane Systems	Germany	Spiral wound
	CSM Membrane operated by Toray Industries	USA	Spiral Wound
	Oasys Water	USA	Proprietary membrane
	Aromatec	Singapore	Hollow fiber developed by Nanyang Technological University in Singapore

Based on the available literature, the mentioned commercial membrane configurations along with lab-made FO membranes tailored to specific applications were all investigated at bench-scale level for various FO applications [28–33]. Moreover, studies on FO membranes have included several pilot-scale demonstrations for the purposes of seawater and brackish water desalination, membrane bioreactor (MBR) effluent, domestic sewage and municipal wastewater treatment [34–40]. For produced water treatment, spiral wound configuration was tested in four pilot-scale FO-based projects [9,41–43]. Looking at the two previously mentioned OC bench-scale studies [11,12], the investigation of the process was performed using CTA-FSh membrane, TFC-FSh and HF membrane modules.
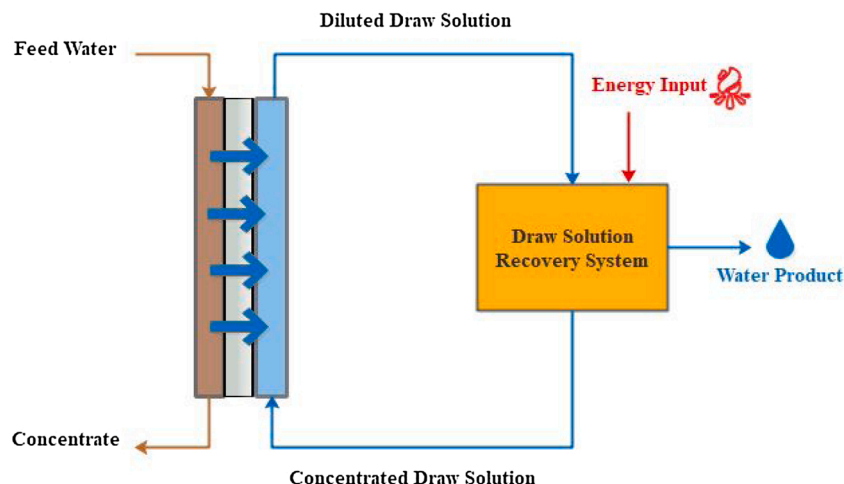

Fig. 1. FO process scheme.

It is widely recognized that the performance of FO-based processes is linked to the operating parameters encompassing feed and draw solutions properties and types, osmotic gradient (i.e. driving force), membrane orientation, cross flow direction, inlet cross flowrate and temperature [44–48]. The influence of these operating parameters can be identified by assessing the feed recovery rate, water flux (L. m^{-2}.h^{-1} (LMH)) and reverse solute flux (mmol. m^{-2}.h^{-1}) as main performance indicators [49,50]. It was proved that there is a positive role of high flowrate and temperature on the FO performance by increasing water flux which was attributed to the reduced concentration polarization and solutions viscosity [45,46,50].

Among all the reported studies evaluating the operating conditions impact on FO systems, few studies were dedicated to examine effect of testing HF membranes on the performance of FO systems under varying conditions [12,51–54]. For instance, Majeed et al. [51] studied the influence of changing flowrates, solutions concentration and membrane orientation on HF membrane obtained from the Korean company Samsung Cheil industries in bench-scale system. They concluded the enhanced performance when DS was facing the active layer, feed and draw solutions were flowing counter-currently and their flowrates were increased. The same study revealed that HF membrane of 0.0396 m^2 achieved 62.9 LMH water flux at the produced osmotic gradient from using deionized water as feed and 2 M NaCl as DS. Another three HF membranes manufactured by the Japanese company Toyobo of 0.12 m^2 area were investigated in bench-scale FO process under different operating parameters [52]. The outcomes were in agreement with Majeed et al. [51] study and the HF membrane was featured with the high water flux. Most importantly of all, Sanahuja-Embuena et al. [55] attempted formulating a testing procedure for HF membrane in a pilot scale FO system at different conditions during operation. Their reported results confirmed that DS concentration is the dominant factor on the membrane performance and the optimum flowrates will diminish the role of membrane orientation.

To the best of the authors' knowledge, there is no reported study that examined the operational performance of HF membrane in pilot-scale OC process for volume reduction of feed water. In this paper, pilot-scale osmotic concentration plant was constructed for reducing the volume of synthetically prepared FS mimicking the process water stream from the oil and gas operations [56]. NaCl solution with salinity comparable to seawater is used as DS. This work highlights the impact of FS, DS flowrates, and operating temperature on the OC operation. DS flowrate was changed at constant FS flowrate. Moreover, the synergetic effect of altering both DS flowrate and temperature is evaluated. The performance of HF membrane at various operating conditions is analyzed mainly from the obtained trends for the feed recovery rates, DS dilution, water flux and reverse solute flux. Lastly, the temperature role on altering the intrinsic properties represented by water and salt permeability coefficients of used HF membrane is also evaluated.

2. Materials and methods

2.1. Materials

2.1.1. Pilot-scale osmotic concentration plant

Pilot-scale FO based osmotic concentration system was constructed for the purpose of the volume reduction of synthetic oil/gas field produced and process water. The schematic diagram of constructed pilot system is shown in Fig. 2 where four tanks with capacity of 5000 L were used for storing the feed solution, draw solution, concentrated feed and diluted draw solutions. The level of water inside the tanks was controlled by installing pressure transmitters (Omega, UK). Two diaphragm pumps (Model KNF Liquiport, Sterlitech, Switzerland) of variable speed were connected to the feed and draw solution tanks for supplying the solutions into the membrane and hence producing the crossflow velocity. Thereafter, the pumped solutions were filtered in two cartridge filters (ATLAS FILTRI, Italy) before entering the membrane to prevent the membrane fouling in case of solid traces existence. The main objective of the unit is to investigate the performance of hollow fiber (HF) FO membrane. Additionally, the plant was ensuring on-line monitoring of flow, pressure and temperature with positioned flowmeters and sensors (Omega, UK). Digital conductivity meters (Model Orion VersaStar Pro, by Thermo Fisher Scientific, US) were used to measure the salinity of the two inlet streams (FS and DS) and the two outlet streams (concentrated FS and diluted DS). The pilot plant encompasses a control panel for all wiring and electrical connections. The system operates automatically after complete programming work done using LabVIEW software (National Instrument, US). The LabVIEW interface screen for operating the system allows the surveillance of pressure, temperature, flow and conductivity along with controlling the inlet FS and DS flowrates. Lastly, the program considers operational safety by setting alarms to detect potential hazards such as high pressure in pipes, high water level in tanks or any leak. Whenever one of the mentioned
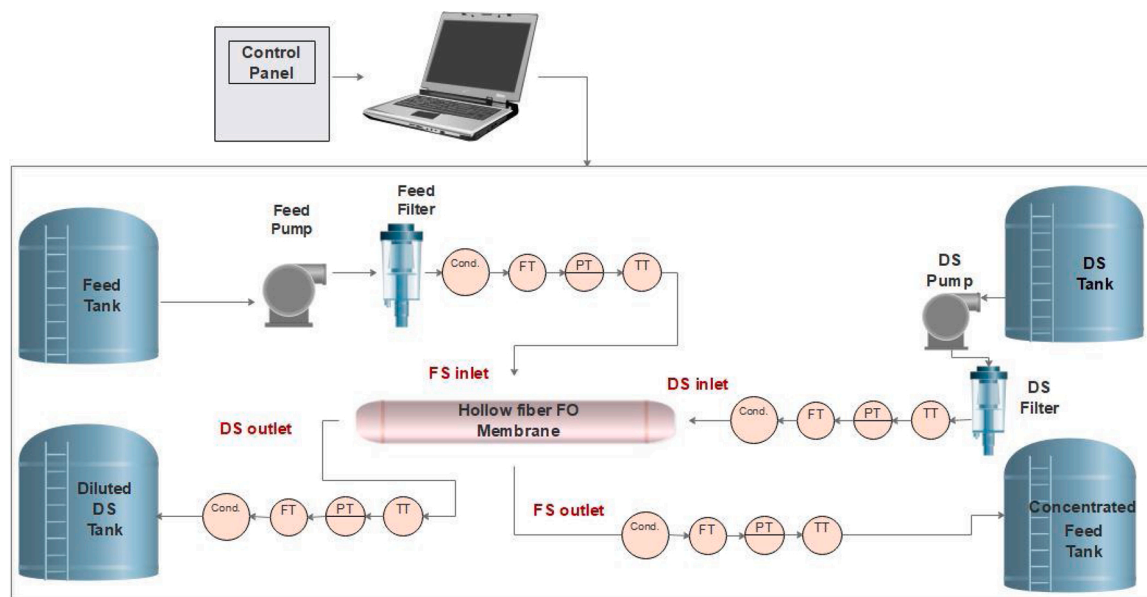

Fig. 2. Schematic diagram of pilot-scale osmotic concentration plant.

parameter deviates from the allowable limit, the pilot-system is automatically switched off.

2.1.2. FO membrane

The utilized FO membrane is commercial HF FO membrane manufactured by Toyobo, Japan. The membrane model is HPC3205 and is produced from the cellulose triacetate (CTA) to offer an enhanced tolerance to chlorine, high efficiency and lower osmotic pressure loss. The tremendous number of fibers placed in the pressure vessel increases the surface area of the membrane and leads to superior performance. The specifications of the membrane are illustrated in Table 2.

2.1.3. Feed and draw solutions

The feed and draw solutions were synthetically prepared from industrial-grade NaCl salt dissolution in tap water. The NaCl salt is received in pellets shape with 20 mm diameter and 10 mm thickness and is manufactured by Concord Overseas in India with 99.62% purity. The tap water was filtered using triple filtration stages filter with one activated carbon and two polypropylene cartridges of 5 microns size (ATLAS FILTRI, Switzerland). The main aim of passing the tap water to the activated carbon cartridge is to assure the removal of chlorine, whereas the two remaining cartridges remove all traces of suspended solids from the tap water. The chlorine in filtered tap water was 0.04 mg.L^{-1} measured using the chlorine kit (HACH, US) and maintained to be lower than the tolerated level by membrane module. The FS was prepared with a salinity of 2000 mg.L^{-1} to mimic Qatari's real process water (PW) being pretreated with membrane bioreactor (MBR). The DS was prepared by dissolving the same industrial-grade NaCl salt in the tap water filtered similarly as in feed solution preparation by (ATLAS FILTRI). The DS concentration is made of 40000 mg.L^{-1} salinity to be comparable with the Arabian Gulf seawater. The characteristics of FS and DS streams are displayed in Table 3.

2.2. Methods

The experiments started by exposing the membrane into countercurrent and once-through flow of feed and draw solutions. The membrane is positioned horizontally with applying the feed solution to the shell side outside the hollow fiber and the draw solution to the bore side inside the hollow fiber (outside-in configuration) as in Fig. 3.

Firstly, the impact of changing the FS flowrate and maintaining constant DS dilution rate of 75% by manipulation with its flowrate were investigated for 4 h of continuous operation at 27 °C. The studied FS
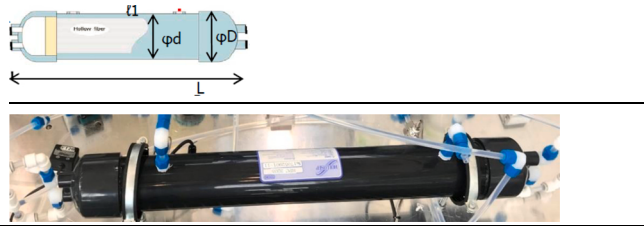
Table 2
HF membrane specifications.

	Membrane Type	Hollow fiber
	OD of hollow fiber	175 μm
Membrane	ID of hollow fiber	85 μm
	Membrane Surface Area	31.5 m^2
	Vessel material	polyvinyl chloride (PVC)
Module	Dimension Φ D, L	103 mm,830 mm
	Φ d, ℓ1	90 mm, 480 mm
	Pressure	Shell side <0.49 MPa, Bore side < 0.2 MPa
Operating Conditions	Temperature	5-40 °C
	pH	3-8
	Residual Chlorine	≤ 1 mg.L^{-1}

Table 3
Feed and draw solutions characteristics.

Parameter (mg.L^{-1})	Feed Solution	Draw Solution
TDS	2000	40000
TSS	1.3	15.2
Inorganic carbon (IC)	18.75	15.4
Total Organic Carbon (TOC)	0.324	0.705
pH	7.90	7.74
Conductivity (mS/cm)	4.0	64.0
Turbidity	0.148	0.719

flowrates are 1.00, 1.35, 1.60 and 2.00 L.min^{-1}. Following that, the impact of changing DS flowrate at constant FS flowrate of 1.10 L.min^{-1} was examined. The chosen DS flowrates were 0.28, 0.35 and 0.45 L.min^{-1} and the process was operated with each flowrate for 2 hours at 27 °C. Additionally, the impact of DS flowrate and seasonal temperature were studied. The same experiment at different DS flowrates conducted during summer at operation temperature of surrounding laboratory of 27 °C were repeated during winter with surrounding temperature of 17 °C. After each experiment, the membrane flushing was done by replacing the inlet DS stream to the membrane with inlet FS stream. Therefore, FS was fed to both sides of membrane for 30 min until both sides approached the same salinity. Above all, the operational stability of the OC pilot-plant was assessed based on conducting long-term experiment for 48 hours of continuous operation. Based on the mentioned FS flowrates, the OC pilot-plant have the potential to run continuously for 1 day and 17 hours at 2.00 L.min^{-1}, and for 3 days and 11 hours at 1.00 L.min^{-1}.

The impact of mentioned operating conditions was studied on OC performance parameters including: feed recovery, DS dilution, water flux and reverse solute flux calculated from the following equations.

$$FR\% = \frac{Q_{F_{in}} - Q_{F_{out}}}{Q_{F_{in}}} \times 100 \tag{1}$$

$$DS\ Dilution\% = \frac{Q_{DS_{out}} - Q_{DS_{in}}}{Q_{DS_{out}}} \times 100 \tag{2}$$

where FR% is the feed recovery percentage, $Q_{F_{in}}$ and $Q_{F_{out}}$ are the volumetric flowrate of feed water inlet and outlet streams respectively. Feed recovery % is the percentage of permeated water in specific time with respect to the initial feed water flowrate and represents the feed concentration % or the volume reduction %. $Q_{DS_{in}}$ and $Q_{DS_{out}}$ are the flowrates of the inlet and outlet DS streams. Whereas, DS Dilution % is the percentage of DS flowrate change per outlet DS stream flowrate including permeated water.

$$J_{W,\ FS} = \frac{Q_{F_{in}} - Q_{F_{out}}}{A_m} \tag{3}$$

$$J_{w,\ DS} = \frac{Q_{DS_{out}} - Q_{DS_{in}}}{A_m} \tag{4}$$

where $J_{W,\ FS}$ and $J_{w,\ DS}$ are the FS water flux and DS water flux respectively (L. m^{-2}.h^{-1} or LMH). $Q_{F_{in}} - Q_{F_{out}}$ is the change in inlet and outlet feed flowrates, $Q_{DS_{out}} - Q_{DS_{in}}$ is the change in inlet and outlet DS flowrates and A_m is the membrane area.

Reverse solute flux (RSF) resulted from the diffusion of DS solutes to the feed side is another parameter of concern during HF membrane testing. The conductivity of solutions detected from the conductivity detectors was transferred into NaCl mass flowrate and overall mass balance assisted in the determination of RSF as:

$$J_s = \frac{(C_{FS_{in}} Q_{FS_{in}} - C_{FS_{out}} Q_{FS_{out}}) \times 60}{A\ Mw_s} \tag{5}$$

where J_s is RSF (mmol. h^{-1}.m^{-2}), $C_{FS_{in}}$ and $C_{FS_{out}}$ are the inlet and outlet feed mass concentrations respectively (mg.L^{-1}), $Q_{FS_{in}}$ and $Q_{FS_{out}}$ are the
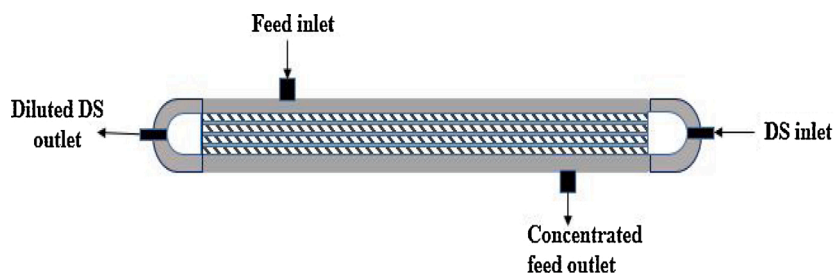
Fig. 3. Outside-in configuration for HF membrane module.

volumetric flowrates of inlet and outlet feed streams respectively (L.min⁻¹), A is the membrane area (m^2) and Mw_s is the solute molecular weight (mg. mmol⁻¹).

Finally, the influence of temperature on the water and salt permeability coefficients of FO membrane was investigated. The membrane was tested at temperature of 20.00, 24.70 and 29.30 °C. The experimental protocol followed to determine the value of coefficient A involve using deionized water as FS, pressurizing the system to 4.9 bar and collecting permeate for 60 seconds. Coefficient A is found according to Eq (6):

$$A = \frac{weight\ of\ permeate\ (kg)}{Membrane\ Area\ (m^2)\ x\ Pressure\ (bar)\ x\ time\ (hour)} \quad (6)$$

The value of coefficient B was calculated from the coefficient A, effective osmotic pressure and salt rejection (R_{NaCl}) correlations.

$$B = A\Delta\pi_{eff}\ \frac{1 - R_{NaCl}}{R_{NaCl}} \quad (7)$$

In addition, the salt rejection (R_{NaCl}) was specified by using 500 mg.L⁻¹ FS, pressurizing the system to 4.9 bar, collecting permeate and measuring conductivity.

$$R_{NaCl} = \left(1 - \frac{Conductivity\ of\ permeate}{Conductivity\ of\ feed}\right) x100\% \quad (8)$$

All sets of experiments were duplicated to check how successful the system is in giving reproducible data. Therefore, experimental outcomes were reproducible with less than 5% error (i.e. difference between the duplicated experiments).

3. Results and discussion

3.1. Effect of feed and draw solutions flowrates

The impact of simultaneous increase of FS and DS flowrate passing through the HF membrane on the performance of OC pilot plant was evaluated at 27 °C. As the aim of the all four conducted experiments at different FS flowrates is maintaining no more than 75% DS dilution, the dilution rate was controlled by DS flowrate alteration at each experiment as shown in Table 4.

It is evident that increasing the FS flowrate requires higher DS flowrate to maintain the 75% dilution. When the initial FS flowrate (1.00 L.min⁻¹) was doubled to 2.00 L.min⁻¹, the DS flowrate was elevated by 21% from 0.33 to 0.40 L.min⁻¹. Besides, adjusting 35% and 60% higher FS flowrate of 1.35 and 1.60 L.min⁻¹ compared to 1.00 L.min⁻¹

Table 4
Required DS flowrate for maintaining 75% DS dilution at each specified FS flowrate.

FS Flowrate (L. min⁻¹)	DS Flowrate (L. min⁻¹)
1.00	0.33
1.35	0.35
1.60	0.37
2.00	0.40

was compensated by 6% and 12% increase in DS flowrate respectively. Above all, the FS flowrate increase was much higher than the corresponding increase in DS flowrate for preserving the same dilution rate.

3.1.1. Feed recovery % (feed volume reduction %)

The achieved feed recovery at each studied FS and DS volumetric flowrates during the entire 4 hours of experimental time is demonstrated in Fig. 4. The figure illustrates the inverse relationship between flowrates and feed recovery %, where adjusting higher flowrates lowers the rate of feed recovery. This relation can be inferred from the equation (Eq. (1)) used to determine the feed recovery.

Fig. 4 shows that maximum feed recovery of 90% was achieved at the lowest studied FS and DS flowrate of 1.00 L.min⁻¹ (LPM) and 0.33 L.min⁻¹ respectively. Increasing both flowrates to 1.35 and 0.35 L.min⁻¹ for FS and DS respectively descended the feed recovery to 75%. Feed recovery % was reduced by 9.3% reaching 68% as a result of FS and DS flowrates elevation to 1.60 and 0.37 L.min⁻¹ respectively. At the highest tested FS and DS flowrates (2 and 0.40 LPM), the feed recovery was further reduced to 60%. The low feed recovery was a consequence of the feed flowrate being higher than the permeate flow rate ($Q_{F_{in}} - Q_{F_{out}}$). The same finding of the FS flowrate effect on the recovery rate was reported in a previous research study using spiral wound FO membrane [46].

3.1.2. Water flux

The impact of changing FS and DS flowrates on the membrane water flux (J_w) was studied at 27 °C during four hours of continuous operation. Fig. 5 (a) clearly illustrates that stable water flux profiles at each tested flowrates during the entire operation time of the pilot-scale system. The stable water flux profiles indicate that DS concentration was not diminished and driving force was maintained throughout the entire operation time. However, the observed flux decline in the first few minutes is attributed to the instability of water flow across both sides of membrane when FS and DS were adjusted.

Fig. 5 (b) demonstrates the average water flux obtained at studied flowrates when experiments were conducted in duplicate along with interpreting the increasing trend with the increase in both FS and DS flowrates. It was found that the flux increased from 1.70 LMH at FS and DS flowrates of 1.00 and 0.33 L.min⁻¹ to 2.20 LMH at FS and DS flowrates of 2.00 and 0.40 L.min⁻¹. This 29.40% flux enhancement was resulted from 100.00% and 21.21% elevation in volumetric flowrate of FS and DS respectively. This indicates that higher volumetric flowrates are advantageous in terms of increasing the water permeation across membrane surface; however, they lower the rate of feed recovery. The 29.40% flux increase from 1.70 to 2.20 LMH was accompanied with 33.33% decline in feed recovery rate from 90.00% to 60.00% as presented in Fig. 4. The obtained flux trend was similar to the trend confirmed in the research of Hawari et al. [45], where the effect of changing both FS and DS flowrates was studied and high water flux of flat sheet thin film composite (TFC) FO membrane was produced at increased volumetric flowrates.

The experimental results have confirmed the direct proportion of flux with the flowrates in which increasing the flowrates yields higher flux. On the other hand, the low flux at reduced FS and DS flowrates
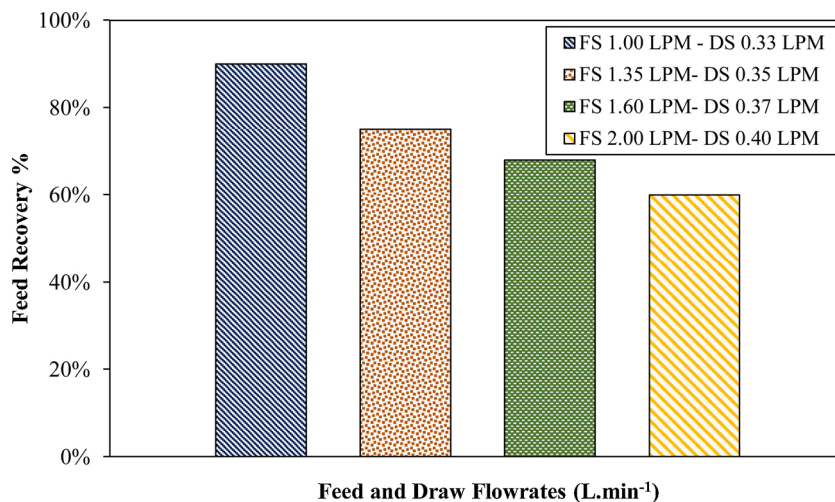
Fig. 4. Effect of increasing FS and DS flowrates on feed recovery percentage at 27 °C.
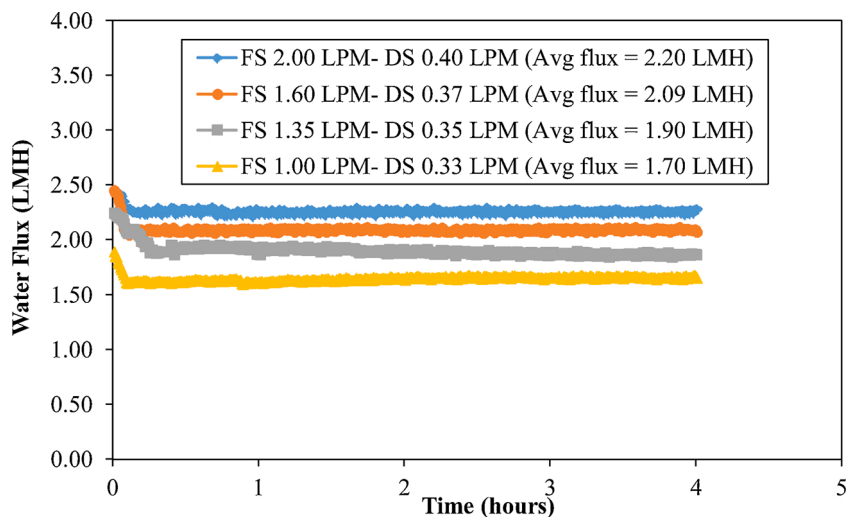

Fig. 5. Effect of changing FS and DS flowrates on the water flux at 27 °C.
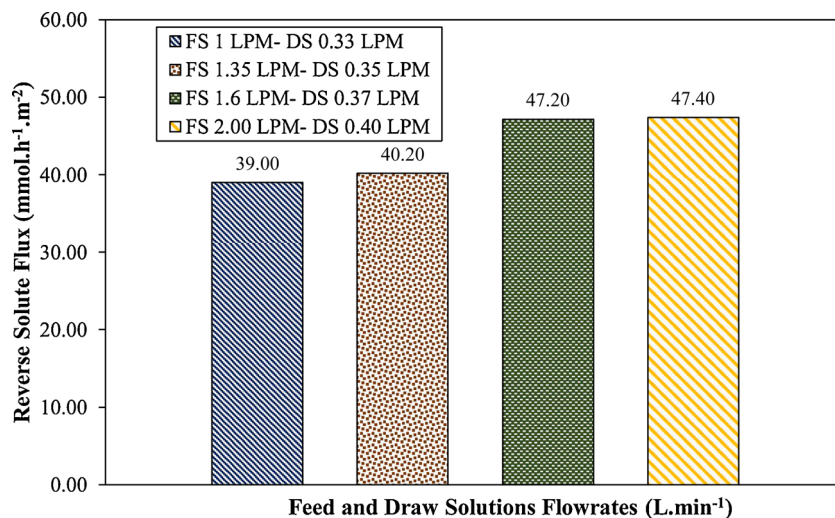

Fig. 6. Effect of changing FS and DS flowrates on the reverse solute flux at 27 °C.

during HF membrane testing was attributed to the concentration polarization (CP) phenomenon. The high flowrates of FS and DS were capable to increase the module turbulence and minimize the effect of CP [50]. For instance, the high water flux obtained was a results of solute accumulation impediment after subjecting the membrane to high FS and DS flowrates [57]. The advantageous role of the high flowrate on both sides of the membrane on enhancing the mass transfer coefficient and increasing the flux was reported and demonstrated by many studies [36, 48,58].

3.1.3. Reverse solute flux

The impact of pilot-scale osmotic concentration unit operation for different feed and draw solutions flowrate on the reverse solute flux (RSF, (J_s)) was also studied during HF membrane module testing at 27 °C during four hours of continuous operation. Actually, the RSF is an indication for salts- NaCl in this case- which flow in reverse from DS to FS and oppose the conventional water flow direction. Higher RSF is not desirable as it reduces the DS concentration, hence accelerates the decline of osmotic driving force and water flux [59]. Aside from the reduced driving force, high RSF rates elevates the periodical needs for replenishing the DS and recovering its high osmotic pressure [60].

Fig. 6 demonstrates that low volumetric flowrates of FS and DS allow less amount of solutes to be transferred from DS to FS side from the shown RSF values. The minimum reverse diffusion of solutes was 39.00 mmol.h^{-1}.m^{-2} at lowest FS and DS tested flowrates and at 27 °C. However, the operation at the highest studied flowrates of FS and DS was characterized by maximum reverse diffusion rate of DS solutes into the feed water. The maximum RSF for HF module at 27 °C was estimated by 47.40 mmol.h^{-1}.m^{-2} that is equivalent to 2770 mg.h^{-1}.m^{-2} of NaCl available in DS reversing their diffusion into FS. This indicates that the DS flow at high rate induced the solutes to diffuse through membrane into the feed. The operation at highest flowrates produces 21.54% higher RSF than the produced at lowest flowrates. Therefore, adjusting low flowrates of FS and DS is preferable to minimize the RSF phenomenon across the HF membrane.

It is obvious from the demonstrated trends that water flux and RSF are directly proportional to each other. It was found that RSF was high at higher adjusted flowrates described by elevated average water flux rather than at lower flowrates. The relationship of water flux and RSF was demonstrated in the research of Heo et al. [61] who studied the RSF trend with water flux for several DS of different concentrations and reported the linear increase in RSF with the water flux increase.

3.2. Effect of DS flowrate at constant feed flowrate

3.2.1. Feed recovery (feed volume reduction) and DS dilution rate

For the adjusted DS flowrates at each performed experiments, the feed recovery rate along with the DS dilution degree were approximated as in Fig. 7. The trends presented are based on average values taken for the entire duration of each experiment. It is evident that elevated DS flowrate has an advantageous influence on increasing the feed recovery rate. Higher DS flowrate enables drawing higher amount of feed water. This suggests that small positive hydraulic pressure could be evolved in the direction of DS rendering higher permeation rate [50]. The experimental results indicate that an overall increasing of DS flowrate by 60.71% contribute to 62.50% increase in feed recovery rate. When FS and DS flowrates were adjusted to 1.10 and 0.28 L.min^{-1} respectively, the osmotic concentration process successfully recovered around 56.00% of feed water. An additional of 50.89% increase in the recovery rate was distinguished when DS flowrate was turned higher into 0.35 L. min^{-1} at the same FS flowrate, rising the recovery rate of feed to around 84.50%. Further increasing the DS flowrate to 0.45 L.min^{-1}, the recovery rate was high reaching around 91.00%.

In addition to the positive relationship demonstrated between the feed recovery and the DS flowrate, Fig. 7 shows the effect of changing DS flowrate on its dilution rate. Throughout all the conducted experiments, the dilution rate of the DS found from Eq. (2) slightly decreased by 7.74% where DS flowrate increase was around 60.71%. Adjusting the FS and DS flowrates to 1.10 and 0.28 L.min^{-1} respectively resulted in diluting the inlet DS stream to have 27.00% of initial salinity (40000 mg. L^{-1}). Increasing the DS flowrate to 0.35 L.min^{-1} decreased the dilution where the outlet diluted DS has salinity around 29.50% of initial DS salinity. At the highest studied DS flowrate (0.45 L.min^{-1}), the DS dilution rate was the lowest where the diluted DS is with 32.65% of initial DS salinity. The slight changes in DS dilution rates and diluted DS salinity resulted at the studied DS flowrates were in the range of the experimental error and were not caused certainly by the DS flowrate.

3.2.2. Water flux

The profiles of water flux with time are shown in Fig. 8 (a) for the three experiments where the influence of DS flowrate used to draw feed water on the permeate water productivity can be observed. The higher the DS flowrate, the higher the permeation rate throughout the entire duration of the experiment. This was inferred by the observed remarkable increase in the water flux when DS flowrate was increased by 60.71% from 0.28 to 0.45 L.min^{-1}. Moreover, the trends illustrate the
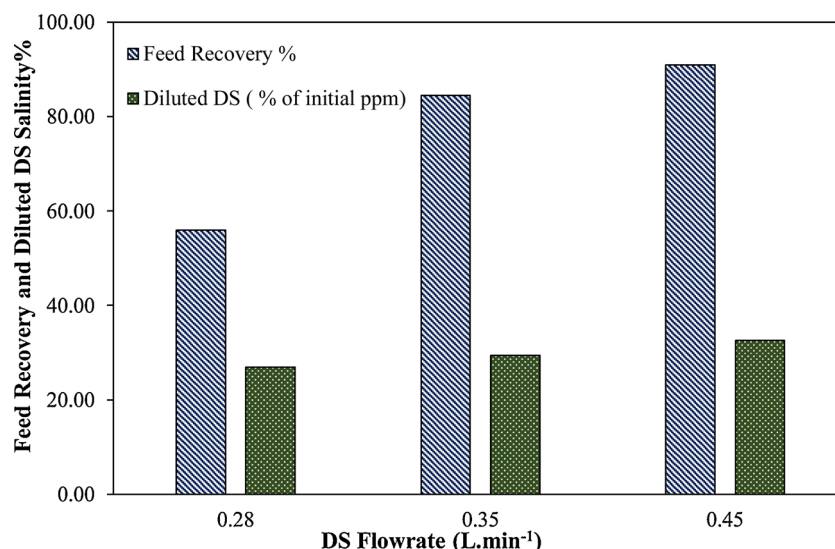

Fig. 7. Effect of increasing DS flowrate on feed recovery and DS dilution rates at 27 °C.
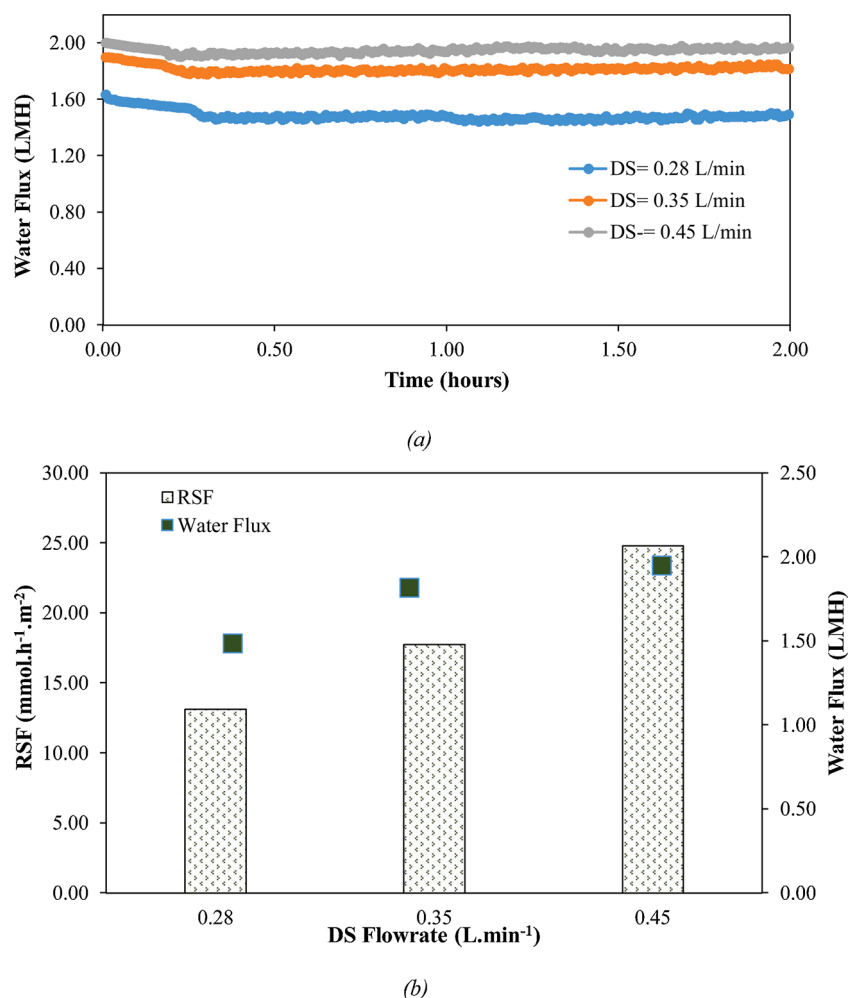
(a)

(b)

Fig. 8. Effect of increasing DS flowrate on the water flux and reverse solute flux at 27 °C.

stable operation of the experiments at the obtained flux during the 2.00 hours. A negligible flux decline was experienced showing insignificant reduction in the osmotic gradient.

The average flux obtained at DS and FS flowrate of 0.28, 1.10 L.min^{-1} respectively is 1.48 LMH and increased by 22.97% to 1.82 LMH when the DS flowrate was increased by 25.00% to 0.35 L.min^{-1} at the same FS flowrate as illustrated in Fig. 8 (b). Particular increase in the DS flowrate to 0.45 L.min^{-1} resulted in raising the average flux to 1.95 LMH. Therefore, the results show an approximate flux enhancement of 31.76% from 1.48 to 1.95 LMH when DS flowrate was increased by 60.71% from 0.28 to 0.45 L.min^{-1}.

The increase in the flux is a result to the high permeation rate induced by the high DS flowrate. This suggests that high DS flowrate generates high cross flow velocity shear force which minimizes the cake enhanced concentration polarization (CECP) and dilution effect [36,46]. Therefore, the flux increases due to the increased driving force after replenishing the concentration of diluted DS at the membrane surface and this findings are in good agreement with the research of Hawari et al. who studied effect of high DS flowrate on water flux [45].

3.2.3. Reverse solute flux

In a similar behavior to the possessed by the water flux, reverse solute diffusion to feed side increases at higher DS flowrates as indicated by the solute flux Fig. 8 (b). Changing the DS flowrate from 0.28 to 0.45 prompted high occurrence of reverse solutes diffusion that was increased from 13.13 to 24.80 mmol.h^{-1}. m^{-2}. For a 25% increase in DS flowrate from 0.28 to 0.35 L.min^{-1}, the RSF increased by 35.11% from

13.13 to 17.74 mmol.h^{-1}. m^{-2}. The maximum reverse diffusion of solutes was determined at 0.45 L.min^{-1} for DS with flux reaching 24.80 mmol.h^{-1}. m^{2}. The determined RSF trend confirms the direct relationship with water flux as explained earlier in section 3.1.3.

3.3. Effect of draw solution flowrate and operating temperature

3.3.1. Feed recovery (feed volume reduction) and DS dilution rate

Fig. 9 shows the effect of both temperature and DS flowrate change on the amount of feed recovered along with the attained DS dilution rate affecting the outlet diluted DS salinity. It is obvious that DS dilution increases at higher temperature which is reflected into lower diluted DS salinity percentage of the initial. Besides, the feed recovery increases with changing both the DS flowrate and the solutions temperature.

For 58.8% and 60.71% increase in the temperature and DS flowrate respectively, the overall achieved feed recovery enhancement is estimated by 84.81%. At the lowest DS flowrate of 0.28 L.min^{-1} and temperature of 17 °C around 49.24% of feed water inlet stream was recovered compared to 91.00% of inlet feed water recovered at the highest DS flowrate of 0.45 L.min^{-1} and temperature of 27 °C. Around 49.24% of feed was recovered at the initial DS flowrate of 0.28 L.min^{-1}, then 66.36% of feed water was recovered when DS flowrate was increased by 25% at the temperature of 17 °C. Following that, feed water recovery was increased by 6.29% where 70.54% of feed water inlet stream was reclaimed at the same temperature. On the other hand, the acquired rates of feed recovery at 27 °C were 56.00%, 84.50% and 91.00% for DS flowrate of 0.28, 0.35 and 0.45 L.min^{-1} respectively being
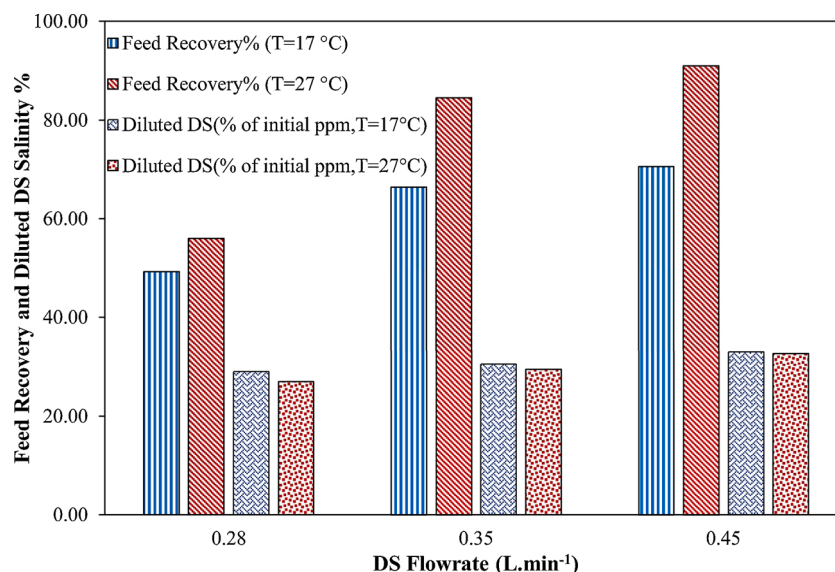
Fig. 9. Comparison between feed recovery and DS dilution rates obtained at different DS flowrates and operation temperatures.

higher at each tested flowrate. This indicates that the elevated feed recovery at the higher temperature is a result to the high amount of water permeated through the membrane. It is reported that increased temperature of the solutions works to alter their thermodynamic properties represented by osmotic pressure, diffusivity and viscosity [62,63]. Therefore, the high water permeation is thought to be a response to the decreased FS and DS solutions' viscosity that allows more diffusivity of water molecules through active and support layers of membrane thereby increases the mass transfer.

Consequently, the high water permeation from FS to DS at high temperature will assure increased dilution rate from the initial concentration of the DS. However, raising the temperature and DS flowrate by the same above-mentioned percentages had slight impact on enhancing the DS dilution compared to feed recovery. At DS flowrate of 0.28 L.min⁻¹, the diluted DS had 6.90% lower salinity when temperature increased from 17 to 27 °C, which confirms obtaining higher DS dilution rate at higher temperature. Additionally, the obtained results show that diluted DS salinity is lowered slightly from 30.50% to 29.50% and from 33% to 32.65% at DS flowrates of 0.35 and 0.45 L.min⁻¹ respectively when the temperature is increased from 17 °C and 27 °C. It is also worth mentioning that the slight changes in DS dilution rates resulted at the studied DS flowrates were in the range of the experimental error and

were not caused certainly by the DS flowrate.

3.3.2. Water flux

Fig. 10 demonstrates that adjusting high DS flowrate has an impact on increasing the amount of water permeates across the membrane area (LMH) at both temperatures. However, proceeding with the experiments during a warmer weather where the laboratory temperature was high supports in obtaining high flux values. The average flux of 0.91 LMH resulted from DS flowrate of 0.28 L.min⁻¹ at temperature of 17 °C is increased by 62.64% when temperature raised by 10 °C. Besides, 25% increase in DS flowrate to 0.35 L.min⁻¹ produced around 22.97% higher water flux estimated by 1.82 LMH at 27 °C rather than the 1.48 LMH generated at 17 °C. The high temperature helped in improving the flux by 20.37% from 1.62 to 1.95 LMH at the highest tested DS flowrate of 0.45 L.min⁻¹.

At the temperature of 17 °C, the flux increased by 78.00% when DS increased by 60.71% from 0.28 to 0.45 L.min⁻¹. The influence of increasing both the DS flowrate from 0.28 to 0.45 L.min⁻¹ and the temperature from 17 to 27 °C is determined by achieving 114.29% enhancement in the overall water flux. The useful role of increasing these two parameters simultaneously on improving the water flux was also confirmed previously [45]. Hawari et al. [45] elucidated around
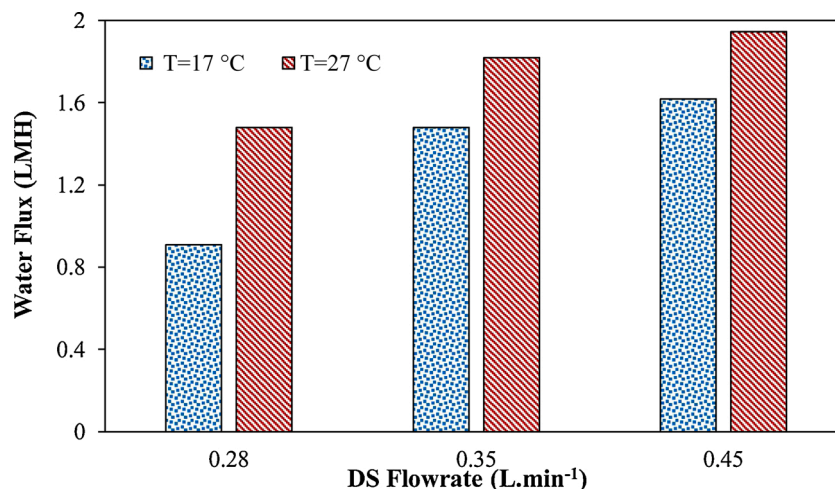

Fig. 10. Comparison between water flux obtained at different DS flowrates and operation temperatures.

93.30% flux improvement when DS flowrate is increased from 1.20 to 3.20 L.min^{-1} with temperature rise by 30% from 20 to 26 °C.

The acquired results indicated the favorable role of the high temperature in producing higher water flux values. The attained trends of flux at a higher temperature was confirmed by previous research studies on the FO process which investigated the temperature influence on the water and solute fluxes [47,57,64–68]. The high temperature of the surrounding leads to increase the temperature of the FS and DS inlet streams to the FO membrane modules. For instance, the direct impact of the temperature change on the osmotic pressure is presented by Van't Hoff's equation, in which any increase in temperature leads to higher osmotic pressure. Subsequently, the flux could be improved due to the enhanced osmotic pressure of solutions and driving force across the membrane. Furthermore, McCutcheon and Elimelech [69] designated the improved flux at high temperatures to the greatly reduced concentration polarization from the high diffusivity of the NaCl solutes. Higher diffusion coefficients of NaCl solutes in FS and DS reduces the impact of external concentration polarization (ECP) and lessens the solute resistivity in the porous layer of the membrane leading to reduced internal concentration polarization (ICP).

3.3.3. Reverse solute flux

The reverse solute flux is known to have linear relation with the water flux as described earlier, thus the improved water flux at higher temperature is accompanied with increased RSF at the same high temperature. The impact of DS flowrate on the RSF was compared for the two temperatures of 17 and 27 °C in Fig. 11. The figure illustrates the higher reverse solute flux obtained for each DS flowrate at the higher temperature. To further explain the increasing trend of RSF with respect to temperature, the ICP is reduced at high temperature due to the less resistivity of NaCl solutes which boosted the back diffusivity of solutes to the feed side [61].

The comparison of the two RSF values obtained at each DS flowrate with respect to temperature yields 40.13%, 35.52% and 23.81% higher RSF for DS flowrate of 0.28, 0.35 and 0.45 L.min^{-1} respectively at temperature of 27 °C. The obtained results indicate a decreasing trend for the flux enhancement at T = 27 °C with the increase in DS flowrate.

3.4. Evaluation of OC performance under tested operating conditions

The impact of changing FS and DS flowrates, DS flowrate at constant FS flowrate and temperature were all investigated on the OC performance. In the first set of studied operating conditions (section 3.1), the results indicated that achieving the highest water flux (2.20 LMH) and RSF (47.20 mmol.h^{-1}. m^{-2}) is accompanied with the minimum feed water recovery rate of 60% at the highest tested flowrates (FS = 2.00 L.min^{-1}

and DS = 0.40 L.min^{-1}). In contrast, it was evident that OC operation at the lowest FS and DS flowrates of 1.00 and 0.33 L.min^{-1} respectively showed the system's capability to recover maximum of 90% while the water flux (1.70 LMH) and RSF (39 mmol.h^{-1}. m^{-2}) were at their minimum values compared to the values at the other tested FS and DS flowrates. Despite the fact that the operation for obtaining high feed recovery % while ensuring sufficiently high water flux is preferable as explained earlier, the performed experiments displayed that the operation at the highest flowrates could lead to increased stress on the membrane fibers and the lowest flowrates could enhance the concentration polarization translated into aggravated fouling [15,50]. Therefore, the operation at intermediate FS and DS flowrates of 1.35 and 0.35 L.min^{-1} respectively can be described by being optimum since the achieved feed recovery % (75%) and water flux (1.90 LMH) are reasonably high enough with lower membrane exposure risk to fouling or feed concentration stress.

For the second set of investigated operating conditions (section 3.2) and for the same mentioned reasons, the operation of OC pilot plant at DS flowrate of 0.35 L.min^{-1} can be depicted by being optimum. The operation at the moderate DS flowrate (0.35 L.min^{-1}) from the studied range (0.28-0.45 L.min^{-1}) succeeded in attaining reasonable feed recovery of 84.5% at an average water flux of 1.82 LMH compared to recovering 91% along with achieving water flux of 1.95 LMH at the highest tested DS flowrate of 0.45 L.min^{-1} which elevates the stress exerted on the membrane. Lastly, it is worth mentioning that the performance of OC process at this moderate DS flowrate of 0.35 L.min^{-1} was preferred when operated at higher temperature of 27 °C as discussed in section 3.3.

3.5. Evaluation of OC performance for long-term operation

The operational stability of the constructed OC pilot plant was evaluated through long-term experiment for 48 hours of continuous operation. The experiment was conducted at the optimum conditions mentioned earlier in section 3.4 which are the intermediate flowrates of 1.35 and 0.35 L.min^{-1} for FS and DS respectively at temperature of 23 °C.

The performance of the OC process during the prolonged operation was assessed based on the obtained water flux trend shown in Fig. 12. The nearly stable water flux indicates a successful operation of the OC pilot-plant for the 48 hours. The initial achieved water flux was around 1.80 LMH and slightly decreased to 1.61 LMH at the end of the operation which can be attributed to the diminished driving force. It is evident that the obtained flux in this case (1.66 LMH) is lower than the obtained water flux of 1.90 LMH in section 3.1.2. The lower water flux is due to the solutions' higher viscosity and lower diffusivity at lower operation temperature (23 °C cf. 27 °C) as discussed earlier.
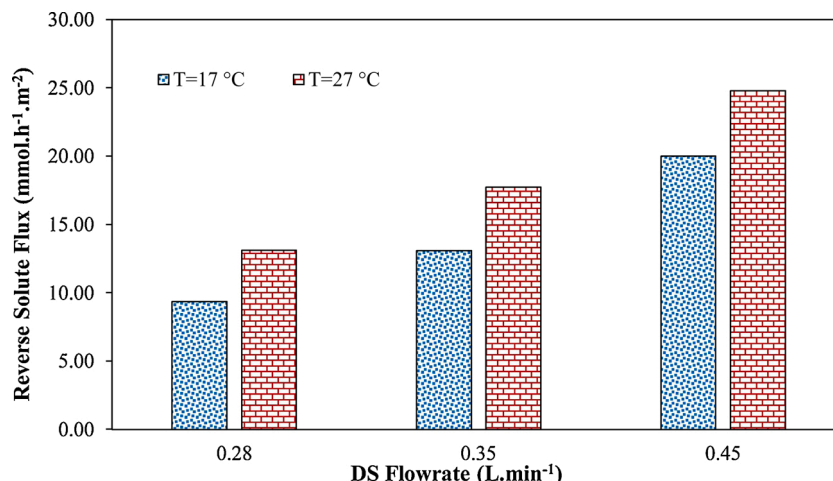

Fig. 11. Comparison between reverse solute flux obtained at different DS flowrates and operation temperatures.
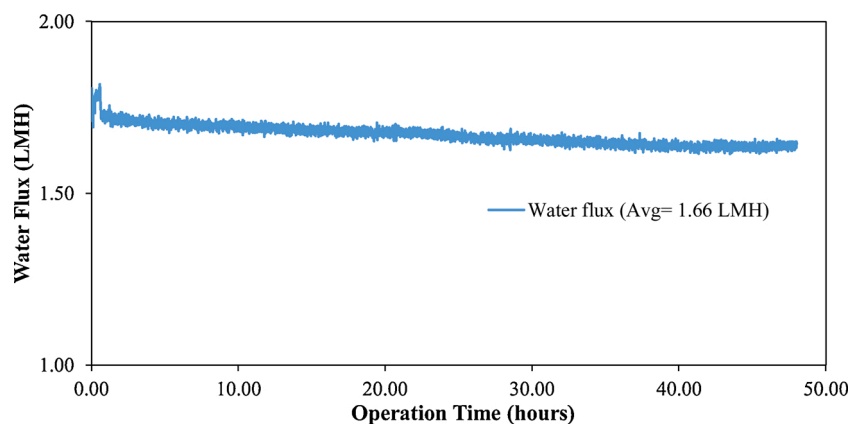
Fig. 12. Water flux trend with time for evaluating the long-term performance of OC pilot-plant.

3.6. Effect of changing temperature on membrane permeability coefficients

The water and salt permeability coefficients (A and B) were determined according to the FO membrane testing protocol explained earlier. The transport parameters of FO membrane (A and B) are considered intrinsic properties since they are independent on the change in some of the operational conditions including flowrates and concentration of DS [67]. In addition, the permeability experiments were performed at different operation temperatures approximated by (20, 24, and 30 °C) to disclose the temperature effect on the permeability evolution. In Fig. 13 the obtained water and salt permeability coefficients (A and B) values are presented for HF membrane. The depicted results demonstrate the high temperature effect on increasing both permeability coefficients. The tememprature effect on the intrinsic properties of several tested FO membranes represented by A and B values also proved the higher permeability coefficients at higher temepratures [63,67,68]. The higher permeability reffered to higher A and B values at elevated temperature is attributed to the enhanced solutions diffusivity and decreased viscosity. Thus, allowing the water and salt to transport through the memrbane's active layer at a higher rate [63].

When temperature is increased by around 46.50% from 20.00 to 29.30 °C the A increased by 30.50% from 0.19 to 0.27 LMH.bar^{-1}. The water permeability coefficient A for the HF membrane relation with temperature fitted a linear model where the coefficient of determination is 0.9994.

$$A = 0.0065 \, T + 0.0666 \qquad (9)$$

The salt permeability coefficient B for the HF membrane experienced slight change with the temperature increase. For instance, the 46.50% temperature elevation had rasied the B by 16.67% and had 13.93% lower impact on B compared to A. Higher coefficient B value indicates the membrane is capable to achieve high salt rejection rates. The attained B values are 0.049, 0.053 and 0.058 LMH at temperature of 20.00, 24.70 and 29.30 °C respectively.

$$B = 0.0009 \, T + 0.0318 \qquad (10)$$

4. Conclusions

The OC process performance of HF membrane was demonstrated at pilot scale for volume reduction of wastewater. Synthetically prepared solutions mimicking process water from Qatari's gas fields' facilities and seawater were used as feed and draw solutions. The impact of changing operating conditions such as feed, draw solutions flowrates and temperature on the performance of the OC pilot-unit was evaluated using HF membrane. Besides, the OC pilot-plant performance on the long-term was assessed through 48 hours of continuous operation. The obtained results showed maximum of 90% feed recovery at the lowest tested FS flowrate of 1.00 L.min^{-1} and DS flowrate of 0.33 L.min^{-1}. Operating the pilot unit at higher FS and DS flowrates resulted in lower feed recovery rates. However, the elevated FS and DS flowrates have boosted the water
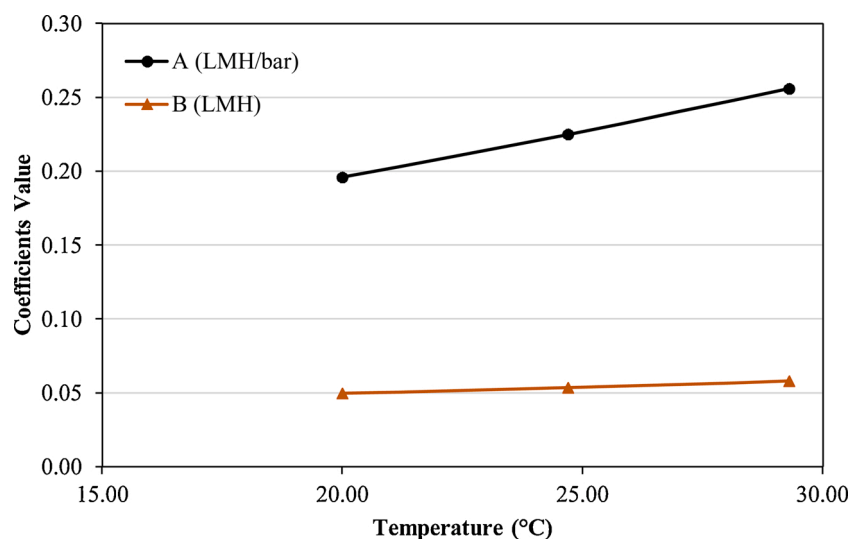

Fig. 13. Effect of increasing temperature on HF membrane permeability coefficients.

flux where maximum flux of 2.20 LMH was attained which is mainly attributed to reduced effect of concentration polarization at higher flowrates. On the other hand, the reverse solute flux increased at higher flowrates due to the enhanced diffusivity of solutes. The operation at intermediate FS and DS flowrates of 1.35 and 0.35 L.min^{-1} respectively can be described by being optimum since reasonably good feed recovery of 75% and water flux of 1.90 LMH were achieved at lower membrane exposure risk to fouling or feed concentration stress. Therefore, the long-term experiment for OC performance evaluation was conducted at these optimum flowrates. Results have indicated successful operation with minimal performance decline at an average water flux of 1.66 LMH. Additionally, it was proved that higher DS flowrate at constant feed flowrate increases the water permeation, the maximum water flux values of 1.95 LMH at DS and FS flowrate of 0.45 and 1.10 L.min^{-1} were obtained at 27 °C. At the highest tested DS flowrate (0.45 L.min^{-1}), the pilot unit was able to recover up to 91 % of feed water. Moreover, the acquired trends have indicated the desirable role of high temperature in improving the feed recovery and water flux as a result of the reduced viscosity and enhanced diffusivity of water; however, it has adverse role in increasing the RSF. At the highest tested DS flowrate (0.45 L.min^{-1}), the water flux was increased from 1.62 LMH (T = 17 °C) to 1.95 LMH (T = 27 °C) and the higher temperature empowered the process to recover around 91% of feed water rather than 70.54% recovery rate achieved at lower temperature. Unfortunately, the lowered resistivity of solutes at the higher temperature (T = 27 °C) boosted the back diffusivity of NaCl solutes to FS side by 23.80%. For this set of experiments, the operation at the moderate DS flowrate (0.35 L.min^{-1}) can be depicted by being optimum along with succeeding in attaining reasonable feed recovery of 84.5% at an average water flux of 1.82 LMH. Lastly, permeability coefficients of HF membrane were improved at higher temperature, maximum reached water and salt permeability coefficients were 0.256 LMH and 0.0581 LMH/bar respectively at 30 °C.

CRediT authorship contribution statement

Rem Jalab: Conceptualization, Data curation, Writing - original draft. **Abdelrahman M. Awad:** Data curation, Formal analysis, Writing - original draft. **Mustafa S. Nasser:** Conceptualization, Supervision, Writing - review & editing. **Joel Minier-Matar:** Formal analysis, Writing - review & editing. **Samer Adham:** Writing - review & editing.

Declaration of Competing Interest

The authors report no declarations of interest.

Acknowledgments

References

[1] B. Van Der Bruggen, P. Luis, Forward osmosis: understanding the hype, Rev. Chem. Eng. 31 (2015) 1–12, https://doi.org/10.1515/revce-2014-0033.
[2] T.S. Chung, L. Luo, C.F. Wan, Y. Cui, G. Amy, What is next for forward osmosis (FO) and pressure retarded osmosis (PRO), Sep. Purif. Technol. 156 (2015) 856–860, https://doi.org/10.1016/j.seppur.2015.10.063.
[3] I.L. Alsvik, M.B. Hägg, Pressure retarded osmosis and forward osmosis membranes: materials and methods, Polymers (Basel) 5 (2013) 303–327, https://doi.org/10.3390/polym5010303.
[4] A.M. Awad, R. Jalab, J. Minier-Matar, S. Adham, M.S. Nasser, S. Judd, The status of forward osmosis technology implementation, Desalination 461 (2019) 10–21.
[5] Q. Ge, M. Ling, T.S. Chung, Draw Solutions for forward osmosis processes: developments, challenges, and prospects for the fututre, J. Membr. Sci. 442 (2013) 225–237, https://doi.org/10.1016/j.memsci.2013.03.046.
[6] S. Munirasu, M.A. Haija, F. Banat, Use of membrane technology for oil field and refinery produced water treatment - a review, Process Saf. Environ. Protein 100 (2016) 183–202, https://doi.org/10.1016/j.psep.2016.01.010.
[7] S. Zhao, L. Zou, C.Y. Tang, D. Mulcahy, Recent developments in forward osmosis: opportunities and challenges, J. Membr. Sci. 396 (2012) 1–21, https://doi.org/10.1016/j.memsci.2011.12.023.
[8] R. Jalab, A.M. Awad, M.S. Nasser, J. Minier-Matar, S. Adham, S.J. Judd, An empirical determination of the whole-life cost of FO-based open-loop wastewater reclamation technologies, Water Res. 163 (2019) 114879, https://doi.org/10.1016/j.watres.2019.114879.
[9] N.R. Hutchings, E.W. Appleton, R.A. McGinnis, Making High Quality Frac Water out of Oilfield Waste, 2011, pp. 19–22, https://doi.org/10.2118/135469-ms.
[10] N.T. Hancock, N.D. Black, T.Y. Cath, A comparative life cycle assessment of hybrid osmotic dilution desalination and established seawater desalination and wastewater reclamation processes, Water Res. 46 (2012) 1145–1154, https://doi.org/10.1016/j.watres.2011.12.004.
[11] K.L. Hickenbottom, N.T. Hancock, N.R. Hutchings, E.W. Appleton, E.G. Beaudry, P. Xu, T.Y. Cath, Forward osmosis treatment of drilling mud and fracturing wastewater from oil and gas operations, Desalination 312 (2013) 60–66, https://doi.org/10.1016/j.desal.2012.05.037.
[12] J. Minier-Matar, A. Santos, A. Hussain, A. Janson, R. Wang, A.G. Fane, S. Adham, Application of hollow fiber forward osmosis membranes for produced and process water volume reduction: an osmotic concentration process, Environ. Sci. Technol. 50 (2016) 6044–6052, https://doi.org/10.1021/acs.est.5b04801.
[13] J. Minier-Matar, A. Hussain, A. Janson, R. Wang, A.G. Fane, S. Adham, Application of forward osmosis for reducing volume of produced/process water from oil and gas operations, Desalination 376 (2015) 1–8, https://doi.org/10.1016/j.desal.2015.08.008.
[14] T.Y. Cath, A.E. Childress, M. Elimelech, Forward osmosis: principles, applications, and recent developments, J. Membr. Sci. 281 (2006) 70–87, https://doi.org/10.1016/j.memsci.2006.05.048.
[15] W.C.L. Lay, T.H. Chong, C.Y. Tang, A.G. Fane, J. Zhang, Y. Liu, Fouling propensity of forward osmosis: investigation of the slower flux decline phenomenon, Water Sci. Technol. 61 (2010) 927–936, https://doi.org/10.2166/wst.2010.835.
[16] M. Perry, How forward osmosis (FO) performance is limited by concentration polarization, ForwardOsmosisTech, 2013 (Accessed August 20, 2019), https://www.forwardosmosistech.com/how-forward-osmosis-performance-is-limited-by-concentration-polarization/.
[17] W. Suwaileh, N. Pathak, H. Shon, N. Hilal, Forward osmosis membranes and processes: a comprehensive review of research trends and future outlook, Desalination 485 (2020) 114455, https://doi.org/10.1016/j.desal.2020.114455.
[18] D.L. Shaffer, J.R. Werber, H. Jaramillo, S. Lin, M. Elimelech, Forward osmosis: where are we now? Desalination 356 (2015) 271–284, https://doi.org/10.1016/j.desal.2014.10.031.
[19] R. Valladares Linares, Z. Li, S. Sarp, S.S. Bucs, G. Amy, J.S. Vrouwenvelder, Forward osmosis niches in seawater desalination and wastewater reuse, Water Res. 66 (2014) 122–139, https://doi.org/10.1016/j.watres.2014.08.021.
[20] Hydration Technology Innovation (HTI), Oil Wastewater Treatment & Gas Wastewater Treatment: Lead Story, 2011 (accessed April 27, 2020), http://www.htiwater.com/divisions/oil-gas/lead_story.html.
[21] Oasys Water, 2020 (n.d.). (accessed April 27,, http://oasyswater.com/solutions/technology/.
[22] Fluid Technology Solutions, Forward Osmosis Membranes for Industrial Applications (n.d.). accessed April 27, 2020, http://ftsh2o.com/products/osmof2o-industrial/.
[23] Aquaporin, Hollow Fiber Forward Osmosis Modules (n.d.). accessed April 27, 2020, https://aquaporin.com/forward-osmosis-membranes/.
[24] TOYOBO, Hollow Fiber Membranes for Industrial Fields (n.d.). accessed April 27, 2020, https://www.toyobo-global.com/seihin/hq/.
[25] Porifera, Membrane Modules (n.d.). accessed April 27, 2020, https://www.porifera.com/modules.
[26] B.D. Coday, P. Xu, E.G. Beaudry, J. Herron, K. Lampi, N.T. Hancock, T.Y. Cath, The sweet spot of forward osmosis: treatment of produced water, drilling wastewater, and other complex and difficult liquid streams, Desalination 333 (2014) 23–35, https://doi.org/10.1016/j.desal.2013.11.014.
[27] S. Chou, L. Shi, R. Wang, C.Y. Tang, C. Qiu, A.G. Fane, Characteristics and potential applications of a novel forward osmosis hollow fiber membrane, Desalination 261 (2010) 365–372, https://doi.org/10.1016/j.desal.2010.06.027.
[28] T. Majeed, F. Lotfi, S. Phuntsho, J.K. Yoon, K. Kim, H.K. Shon, Performances of PA hollow fiber membrane with the CTA flat sheet membrane for forward osmosis process, Desalin. Water Treat. 53 (2015) 1744–1754, https://doi.org/10.1080/19443994.2013.859103.
[29] L. Xia, M.F. Andersen, C. Hélix-Nielsen, J.R. McCutcheon, Novel commercial aquaporin flat-sheet membrane for forward osmosis, Ind. Eng. Chem. Res. 56 (2017) 11919–11925, https://doi.org/10.1021/acs.iecr.7b02368.
[30] C. Bae, K. Park, H. Heo, D.R. Yang, Quantitative estimation of internal concentration polarization in a spiral wound forward osmosis membrane module compared to a flat sheet membrane module, Korean J. Chem. Eng. 34 (2017) 844–853, https://doi.org/10.1007/s11814-016-0307-z.
[31] R.C. Ong, T.S. Chung, J.S. de Wit, B.J. Helmer, Novel cellulose ester substrates for high performance flat-sheet thin-film composite (TFC) forward osmosis (FO) membranes, J. Membr. Sci. 473 (2015) 63–71, https://doi.org/10.1016/j.memsci.2014.08.046.

[32] B.D. Coday, N. Almaraz, T.Y. Cath, Forward osmosis desalination of oil and gas wastewater: Impacts of membrane selection and operating conditions on process performance, J. Membr. Sci. 488 (2015) 40–55, https://doi.org/10.1016/j.memsci.2015.03.059.

[33] G. Han, Z.L. Cheng, T.S. Chung, Thin-film composite (TFC) hollow fiber membrane with double-polyamide active layers for internal concentration polarization and fouling mitigation in osmotic processes, J. Membr. Sci. 523 (2017) 497–504, https://doi.org/10.1016/j.memsci.2016.10.022.

[34] A. Al-zuhairi, A.A. Merdaw, S. Al-aibi, M. Hamdan, P. Nicoll, A.A. Monjezi, S. Al-aswad, H.B. Mahood, M. Aryafar, A.O. Sharif, Forward Osmosis desalination from labratory to market, Water Sci. Technol. (2015), https://doi.org/10.2166/ws.2015.038.

[35] Y. Chun, F. Zaviska, S.J. Kim, D. Mulcahy, E. Yang, I.S. Kim, L. Zou, Fouling characteristics and their implications on cleaning of a FO-RO pilot process for treating brackish surface water, Desalination 394 (2016) 91–100, https://doi.org/10.1016/j.desal.2016.04.026.

[36] J.E. Kim, S. Phuntsho, F. Lotfi, H.K. Shon, Investigation of pilot-scale 8040 FO membrane module under different operating conditions for brackish water desalination, Desalin. Water Treat. 53 (2015) 2782–2791, https://doi.org/10.1080/19443994.2014.931528.

[37] B. Corzo, T. de la Torre, C. Sans, R. Escorihuela, S. Navea, J.J. Malfeito, Long-term evaluation of a forward osmosis-nanofiltration demonstration plant for wastewater reuse in agriculture, Chem. Eng. J. 338 (2018) 383–391, https://doi.org/10.1016/j.cej.2018.01.042.

[38] N.T. Hancock, P. Xu, M.J. Roby, J.D. Gomez, T.Y. Cath, Towards direct potable reuse with forward osmosis : technical assessment of long-term process performance at the pilot scale, J. Membr. Sci. 445 (2013) 34–46, https://doi.org/10.1016/j.memsci.2013.04.056.

[39] R.W. Holloway, A.S. Wait, A. Fernandes da Silva, J. Herron, M.D. Schutter, K. Lampi, T.Y. Cath, Long-term pilot scale investigation of novel hybrid ultrafiltration-osmotic membrane bioreactors, Desalination 363 (2015) 64–74, https://doi.org/10.1016/j.desal.2014.05.040.

[40] L. Chekli, J. Eun, I. El, Y. Kim, S. Phuntsho, S. Li, N. Ghaffour, T. Leiknes, H. Kyong, Fertilizer drawn forward osmosis process for sustainable water reuse to grow hydroponic lettuce using commercial nutrient solution, Sep. Purif. Technol. 181 (2017) 18–28, https://doi.org/10.1016/j.seppur.2017.03.008.

[41] B.D. Coday, T.Y. Cath, Forward osmosis: novel desalination of produced water and fracturing flowback, J. Am. Water Works Assoc. 106 (2014) 37–38, https://doi.org/10.5942/jawwa.2014.106.0016.

[42] R.A. Maltos, J. Regnery, N. Almaraz, S. Fox, M. Schutter, T.J. Cath, M. Veres, B.D. Coday, T.Y. Cath, Produced water impact on membrane integrity during extended pilot testing of forward osmosis – reverse osmosis treatment, Desalination 440 (2018) 99–110, https://doi.org/10.1016/j.desal.2018.02.029.

[43] R.L. McGinnis, N.T. Hancock, M.S. Nowosielski-Slepowron, G.D. McGurgan, Pilot demonstration of the NH3/CO2 forward osmosis desalination process on high salinity brines, Desalination 312 (2013) 67–74, https://doi.org/10.1016/j.desal.2012.11.032.

[44] S. Phuntsho, S. Sahebi, T. Majeed, F. Lotfi, J.E. Kim, H.K. Shon, Assessing the major factors affecting the performances of forward osmosis and its implications on the desalination process, Chem. Eng. J. 231 (2013) 484–496, https://doi.org/10.1016/j.cej.2013.07.058.

[45] A.H. Hawari, N. Kamal, A. Altaee, Combined influence of temperature and flow rate of feeds on the performance of forward osmosis, Desalination 398 (2016) 98–105, https://doi.org/10.1016/j.desal.2016.07.023.

[46] S.J. Im, G.W. Go, S.H. Lee, G.H. Park, A. Jang, Performance evaluation of two-stage spiral wound forward osmosis elements at various operation conditions, Desalin. Water Treat. 57 (2016) 24583–24594, https://doi.org/10.1080/19443994.2016.1157989.

[47] S. Phuntsho, S. Vigneswaran, J. Kandasamy, S. Hong, S. Lee, H.K. Shon, Influence of temperature and temperature difference in the performance of forward osmosis desalination process, J. Membr. Sci. 415–416 (2012) 734–744, https://doi.org/10.1016/j.memsci.2012.05.065.

[48] S. Chakrabortty, M. Pal, M. Roy, P. Pal, Water treatment in a new flux-enhancing, continuous forward osmosis design: Transport modelling and economic evaluation towards scale up, Desalination 365 (2015) 329–342, https://doi.org/10.1016/j.desal.2015.03.020.

[49] S.J. Im, S. Jeong, A. Jang, Feasibility evaluation of element scale forward osmosis for direct connection with reverse osmosis, J. Membr. Sci. 549 (2018) 366–376, https://doi.org/10.1016/j.memsci.2017.12.027.

[50] M.S. Thabit, A.H. Hawari, M.H. Ammar, S. Zaidi, G. Zaragoza, A. Altaee, Evaluation of forward osmosis as a pretreatment process for multi stage flash seawater desalination, Desalination 461 (2019) 22–29, https://doi.org/10.1016/j.desal.2019.03.015.

[51] T. Majeed, S. Phuntsho, S. Sahebi, J.E. Kim, J.K. Yoon, K. Kim, H.K. Shon, Influence of the process parameters on hollow fiber-forward osmosis membrane performances, Desalin. Water Treat. 54 (2015) 817–828, https://doi.org/10.1080/19443994.2014.916232.

[52] M. Shibuya, M. Yasukawa, T. Takahashi, T. Miyoshi, M. Higa, H. Matsuyama, Effect of operating conditions on osmotic-driven membrane performances of cellulose triacetate forward osmosis hollow fiber membrane, Desalination 362 (2015) 34–42, https://doi.org/10.1016/j.desal.2015.01.031.

[53] F. Lotfi, S. Phuntsho, T. Majeed, K. Kim, D.S. Han, A. Abdel-Wahab, H.K. Shon, Thin film composite hollow fibre forward osmosis membrane module for the desalination of brackish groundwater for fertigation, Desalination 364 (2015) 108–118, https://doi.org/10.1016/j.desal.2015.01.042.

[54] S. Zhao, J. Minier-Matar, S. Chou, R. Wang, A.G. Fane, S. Adham, Gas field produced/process water treatment using forward osmosis hollow fiber membrane: membrane fouling and chemical cleaning, Desalination 402 (2017) 143–151, https://doi.org/10.1016/j.desal.2016.10.006.

[55] V. Sanahuja-Embuena, G. Khensir, M. Yusuf, M.F. Andersen, X.T. Nguyen, K. Trzaskus, M. Pinelo, C. Helix-Nielsen, Role of operating conditions in a pilot scale investigation of hollow fiber forward osmosis membrane modules, Membranes (Basel) 9 (2019), https://doi.org/10.3390/membranes9060066.

[56] S. Adham, A. Hussain, J. Minier-Matar, A. Janson, R. Sharma, Membrane applications and opportunities for water management in the oil & gas industry, Desalination 440 (2018) 2–17, https://doi.org/10.1016/j.desal.2018.01.030.

[57] J.R. McCutcheon, M. Elimelech, Influence of concentrative and dilutive internal concentration polarization on flux behavior in forward osmosis, J. Membr. Sci. 284 (2006) 237–247, https://doi.org/10.1016/j.memsci.2006.07.049.

[58] Y.C. Kim, S.J. Park, Experimental study of a 4040 spiral-wound forward-osmosis membrane module, Environ. Sci. Technol. 45 (2011) 7737–7745, https://doi.org/10.1021/es202175m.

[59] S. Lee, C. Boo, M. Elimelech, S. Hong, Comparison of fouling behavior in forward osmosis (FO) and reverse osmosis (RO), J. Membr. Sci. 365 (2010) 34–39, https://doi.org/10.1016/j.memsci.2010.08.036.

[60] N. Akther, A. Sodiq, A. Giwa, S. Daer, H.A. Arafat, S.W. Hasan, Recent advancements in forward osmosis desalination: a review, Chem. Eng. J. 281 (2015) 502–522, https://doi.org/10.1016/j.cej.2015.05.080.

[61] J. Heo, K.H. Chu, N. Her, J. Im, Y.G. Park, J. Cho, S. Sarp, A. Jang, M. Jang, Y. Yoon, Organic fouling and reverse solute selectivity in forward osmosis: role of working temperature and inorganic draw solutions, Desalination 389 (2016) 162–170, https://doi.org/10.1016/j.desal.2015.06.012.

[62] S.J. You, X.H. Wang, M. Zhong, Y.J. Zhong, C. Yu, N.Q. Ren, Temperature as a factor affecting transmembrane water flux in forward osmosis: steady-state modeling and experimental validation, Chem. Eng. J. 198–199 (2012) 52–60, https://doi.org/10.1016/j.cej.2012.05.087.

[63] M.R. Chowdhury, J.R. McCutcheon, Elucidating the impact of temperature gradients across membranes during forward osmosis: coupling heat and mass transfer models for better prediction of real osmotic systems, J. Membr. Sci. 553 (2018) 189–199, https://doi.org/10.1016/j.memsci.2018.01.004.

[64] T.Y. Cath, M. Elimelech, J.R. McCutcheon, R.L. McGinnis, A. Achilli, D. Anastasio, A.R. Brady, A.E. Childress, I.V. Farr, N.T. Hancock, J. Lampi, L.D. Nghiem, M. Xie, N.Y. Yip, Standard methodology for evaluating membrane performance in osmotically driven membrane processes, Desalination 312 (2013) 31–38, https://doi.org/10.1016/j.desal.2012.07.005.

[65] M. Xie, W.E. Price, L.D. Nghiem, M. Elimelech, Effects of feed and draw solution temperature and transmembrane temperature difference on the rejection of trace organic contaminants by forward osmosis, J. Membr. Sci. 438 (2013) 57–64, https://doi.org/10.1016/j.memsci.2013.03.031.

[66] J.G. Lee, N. Ghaffour, Predicting the performance of large-scale forward osmosis module using spatial variation model: effect of operating parameters including temperature, Desalination 469 (2019), https://doi.org/10.1016/j.desal.2019.114095.

[67] Q. Wang, Z. Zhou, J. Li, Q. Tang, Y. Hu, Modeling and measurement of temperature and draw solution concentration induced water flux increment efficiencies in the forward osmosis membrane process, Desalination 452 (2019) 75–86, https://doi.org/10.1016/j.desal.2018.11.001.

[68] L. Feng, L. Xie, G. Suo, X. Shao, T. Dong, Influence of temperature on the performance of forward osmosis using ammonium bicarbonate as draw solute, Trans. Tianjin Univ. 24 (2018) 571–579, https://doi.org/10.1007/s12209-018-0159-1.

[69] J.R. McCutcheon, R.L. McGinnis, M. Elimelech, Desalination by ammonia-carbon dioxide forward osmosis: Influence of draw and feed solution concentrations on process performance, J. Membr. Sci. 278 (2006) 114–123, https://doi.org/10.1016/j.memsci.2005.10.048.